

# Recrystallization Experiments in Tensile Deformed $\langle 100 \rangle$ - and $\langle 111 \rangle$ -Oriented Copper Single Crystals

U. KLEMENT, F. ERNST and P.-J. WILBRANDT

*Institut für Metallphysik der Universität Göttingen, Hospitalstraße 3–5, D-3400  
Göttingen*

(Received 23 July 1987)

Dedicated to the memory of Professor Günter Wassermann

$\langle 100 \rangle$ - and  $\langle 111 \rangle$ -oriented copper single crystals were tensile deformed to a final strain of 20% and 4%, respectively. Specimens prepared from these crystals were abraded at one end. During the subsequent annealing treatment (750 K, 2 h for the  $\langle 100 \rangle$ -oriented crystals and 750 K, 90 min for the  $\langle 111 \rangle$ -oriented crystals) the recrystallization process started on this side. In both cases the orientation relationships between the largest recrystallized grains and the uniformly oriented deformed microstructure can be characterized by the following relations: 22.6°  $\langle 100 \rangle$ , 21.8°  $\langle 111 \rangle$ , 46.8°  $\langle 111 \rangle$  and 129.8°  $\langle 540 \rangle$ . Additionally, in the  $\langle 111 \rangle$  crystals other orientation relationships were found. This is caused by the different dislocation densities in the specimens. The  $\langle 111 \rangle$ -oriented crystals represent the early stage of recrystallization whereas the  $\langle 100 \rangle$ -oriented crystals show the orientations of the late recrystallization stage. Between these stages a further selection of orientations occur.

**KEY WORDS:** Recrystallization, copper, single crystals, orientation relationship.

## INTRODUCTION

During the last years many efforts were made to get a more comprehensive understanding of the mechanisms controlling the development of the recrystallization texture (Lücke, 1984). Nowadays it has been understood that the new orientations are created by annealing twin formation (Berger, 1981; Berger, 1986; Gottstein,

1978; Plege, 1986; Wilbrandt, 1978; Wilbrandt and Haasen, 1980). Yet it remains still uncertain, which of the new orientations will finally dominate in the recrystallized microstructure. This information can be gained only with difficulties from recrystallization experiments in polycrystalline materials. Their deformed microstructure is always very complicated and, frequently, the recrystallized grain grows into differently oriented regions.

Our motivation was to investigate the recrystallization process in a particularly simple deformed microstructure. A suitable microstructure was created by tensile deformation of  $\langle 100 \rangle$ - and  $\langle 111 \rangle$ -deformed copper single crystals. As described elsewhere (Göttler, 1973; Vorbrugg *et al.*, 1971) the orientations of the crystals are stable during the tensile deformation. Therefore specimens of deformed material without any deformation inhomogeneities could be prepared. The homogeneity allows the determination of the orientation relationships between recrystallized grains and the deformed material without any deformation inhomogeneities could be prepared. The homogeneity allows the determination of the one end. The preferred growth direction is fixed by the crystal orientation.

## EXPERIMENTAL

Cylindrical  $\langle 100 \rangle$ - and  $\langle 111 \rangle$ -oriented single crystal of 99.9998% copper of 1 cm in diameter and a length of 15 cm were grown in graphite molds by the Bridgman technique. Additional  $\langle 100 \rangle$ -oriented single crystals were grown from copper of a second charge of the same nominal purity. The crystal axes deviated less than 1° from  $\langle 100 \rangle$  and  $\langle 111 \rangle$ , respectively. The crystals were tensile deformed with an elongation velocity of 0.5 mm/min up to 20% and 4% elongation, respectively. Using spark erosion the deformed crystals were cut into halves. The cutting planes were (100) and (112), respectively. The specimens were about 5 cm and 3 cm in length. Chemical etching for some minutes removed the surface layer disturbed by spark erosion. Then one end was abraded with silicon-carbide paper (grid 120). Annealing was performed in a furnace in an argon atmosphere at 750 K. The annealing time was

2 h for the  $\langle 100 \rangle$ -specimens and 90 minutes for the  $\langle 111 \rangle$ -specimens. Under these annealing conditions only abraded specimens recrystallize. For the metallographic investigations the specimens were etched in  $\text{HNO}_3$  diluted with water.

The orientation of all recrystallized grains with a diameter of more than 3 mm at the surface were determined by the Laue back reflection technique. Thanks to the high precision of determining the cutting plane and evaluation of Laue diagrams, the error in orientation determination is regarded to be less than  $3^\circ$  for the deformed microstructure and less than  $1^\circ$  for the recrystallized microstructure.

## RESULTS AND EVALUATION METHODS

### The deformed microstructure

The slip planes and slip directions of Cu single crystals oriented for tensile deformation in  $\langle 100 \rangle$  or  $\langle 111 \rangle$  direction are shown in Figure 1. There are 8 or 6 equally favoured systems, respectively. The microstructure of  $\langle 100 \rangle$ -oriented tensile deformed Cu single crystals has been described in detail by Göttler (1973). Investigations of the

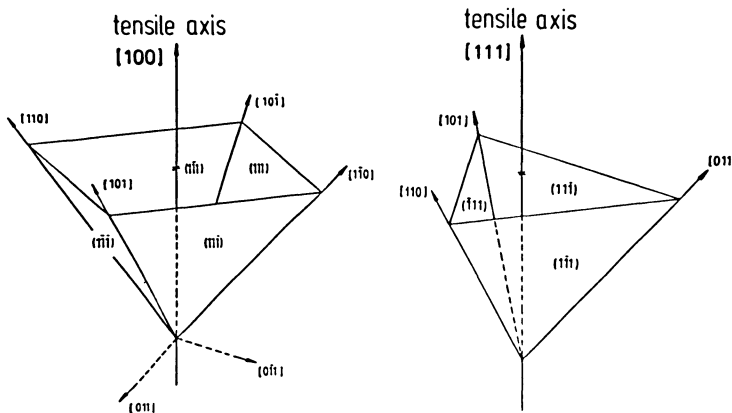


**Figure 1** Slip planes and slip dislocations of the  $\langle 100 \rangle$ - and  $\langle 111 \rangle$ -oriented crystals.

deformation behaviour and the dislocation arrangements of  $\langle 111 \rangle$ -oriented single crystals described elsewhere (Göttler, 1973; Pfeiffer, 1964; Vorbrugg *et al.*, 1971) showed that the  $\langle 111 \rangle$ -oriented single crystals have a similar microstructure as the  $\langle 100 \rangle$ -oriented ones. For both tensile directions, the deformed microstructure consists of

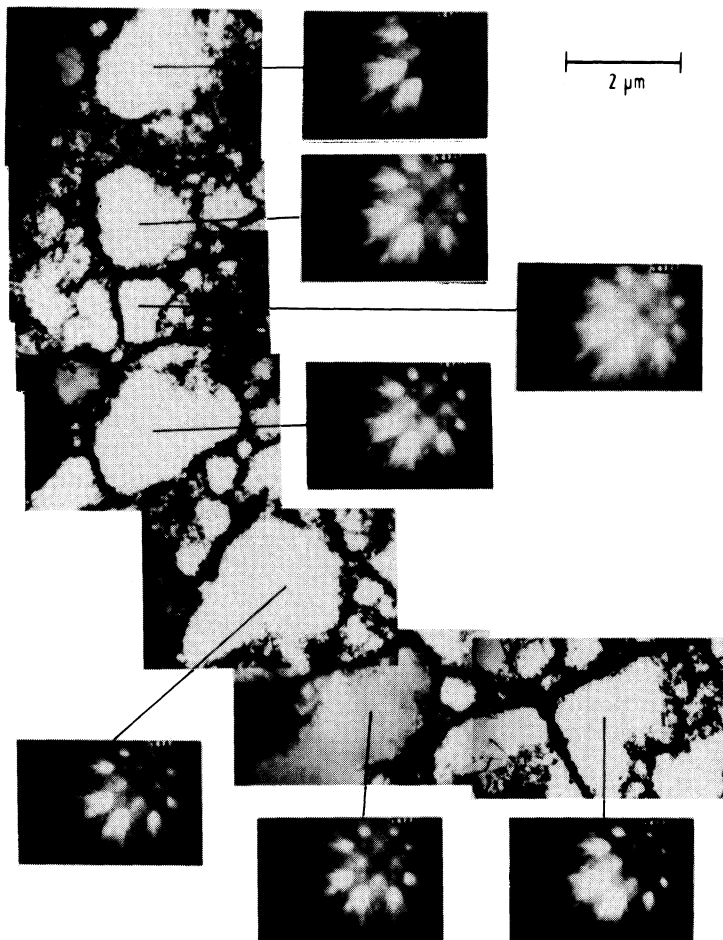


**Figure 2** TEM-micrograph of the deformed microstructure of a  $\langle 100 \rangle$ -oriented copper single crystal 20% deformed. The diffraction patterns show the orientations of the marked subgrains.

nearly identically oriented dislocation free cells separated by dislocation walls. Figure 2 shows a TEM micrograph of the microstructure of a deformed  $\langle 100 \rangle$ -oriented crystal (elongation 20%). As can be seen in the micrograph, the typical cell diameter is about  $1.5 \mu\text{m}$ . The dislocation-rich cell walls are about  $0.25 \mu\text{m}$  thick. The additional diffraction patterns present the orientations of different cells. Their identical appearance demonstrate the extremely small orientation scatter within the whole specimen. The orientation difference between adjacent subgrains is less than  $1^\circ$ . So the orientation scatter within the whole specimen is estimated as less than  $2^\circ$ . According to Göttler (1973) the arrangement of subgrains shows no preferred directions. The assumption of an isotropic density of the stored elastic energy is therefore justified. The dislocation density of the  $\langle 100 \rangle$ -oriented crystals after 20% deformation can be calculated as  $4.5 \cdot 10^{10} \text{ cm}^{-2}$  according to Göttler (1973) and Vorbrugg, Goetting and Schwink (1971). A 4% elongation of the  $\langle 111 \rangle$ -oriented crystals produces a less pronounced cell structure. Yet the scatter of orientations is as small as in the  $\langle 100 \rangle$ -oriented crystals. According to Ambrosi, Göttler and Schwink (1974) the dislocation density in these specimens is  $1.0 \cdot 10^{10} \text{ cm}^{-2}$ .

### Metallography of the recrystallized microstructure

Typical examples of the microstructure of a recrystallized  $\langle 100 \rangle$ - and  $\langle 111 \rangle$ -specimen are shown in Figure 3. The grain size is small at the abraded end and grows with increasing distance from that end. The largest grains are some cm in length. The recrystallized microstructure contains numerous annealing twins which are easily visible because of their straight traces of coherent twin boundaries at the surface. The additional  $\langle 100 \rangle$  crystals (grown from copper of the second charge) show a similar microstructure. Yet the average grain size is a factor of two smaller.

Contrary to the  $\langle 100 \rangle$ -specimens the  $\langle 111 \rangle$ -specimens recrystallize only partially during the annealing treatment. This results from the lower dislocation density in the  $\langle 111 \rangle$ -deformed material. Moreover, in this kind of specimen many small twin lamellae are visible resulting from orientation changes by twinning and back-twinning.

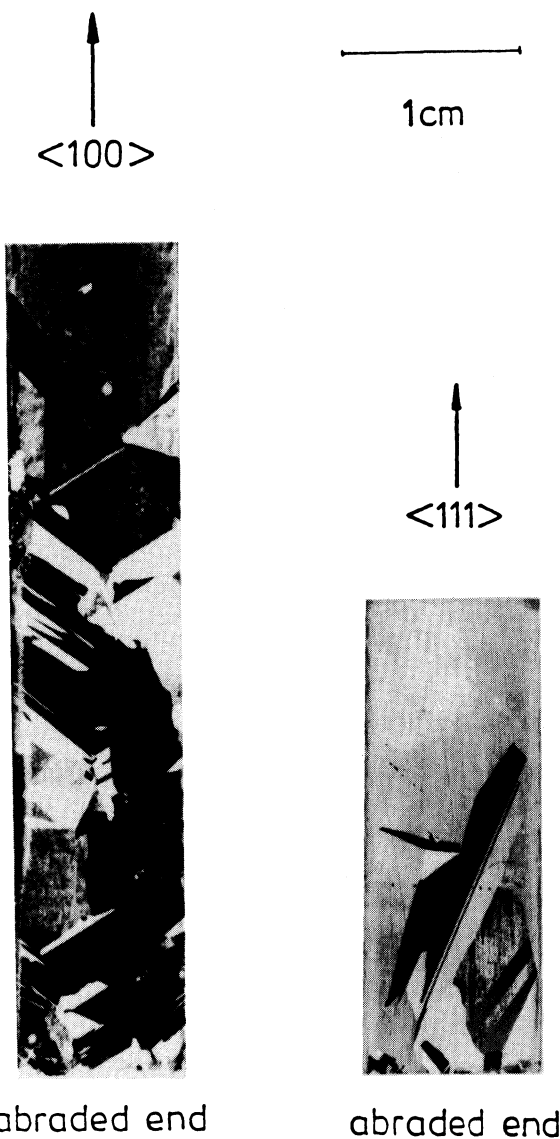


**Figure 3** Recrystallized microstructure of  $\langle 100 \rangle$ - and  $\langle 111 \rangle$ -oriented specimens.

### Orientations of the recrystallized grains

In this section the further evaluation of the measured orientation manifold of the recrystallized grains will be explained in detail. First, the orientation relationships between the orientations of the recrystallized grains and the deformed microstructure are determined. A system of idealized orientation relation-types has been established in order to give a crystallographically interpretable and accurate description for the manifold of the observed orientation relationships. An orientation relationship  $w[hkl]$  is considered to be of the type  $s\langleuvw\rangle$  if the deviation between the observed and the idealized rotation axis does not exceed a maximum value of  $10^\circ$ . Because of the symmetry of the fcc-lattice every observed orientation relationship has 24 equivalent  $w\langle hkl \rangle$  descriptions. In order to get an idea about dominant orientation relation-types with low indexed rotation axes only the rotation angles  $w$  of those of the 24  $w\langle hkl \rangle$  descriptions with  $\langle hkl \rangle$  close to  $\langle 100 \rangle$ ,  $\langle 110 \rangle$  or  $\langle 111 \rangle$  were investigated for each of the measured orientations. For rotations about these three axes the observed frequencies of occurrence of rotation angles are presented in the histograms in Figures 4 and 5.

The histograms represent all of the 70 measured orientation relationships of the  $\langle 100 \rangle$ -specimens and 74 of the 99 orientation relationships observed in the  $\langle 111 \rangle$ -specimens. Unequivocally, the rotation angles are not randomly distributed. The  $\langle 100 \rangle$ -specimens show more pronounced frequency maxima than the rotation angle distribution of the  $\langle 111 \rangle$ -specimens. In Table 1 the preferred rotation angles for the three axes are listed. Taking into account the symmetry of the fcc-lattice the rotation angles can be reduced to the crystallographic equivalent values. They are tabulated in the third column of the table.

A further investigation of the orientation relationships of the  $\langle 100 \rangle$  specimens yields that for the  $\langle 110 \rangle$ -axis the deviations between observed and idealized axis are generally larger than for the  $\langle 100 \rangle$ - and  $\langle 111 \rangle$ -axes. Moreover, especially for the  $\langle 110 \rangle$ -axis the distribution is not as sharp as the other ones. In order to get a more accurate idealization, the rotation axis was calculated by averaging the corresponding components of the observed rotation axis. It turns out that  $\langle 430 \rangle$  is a better idealization. Using this axis

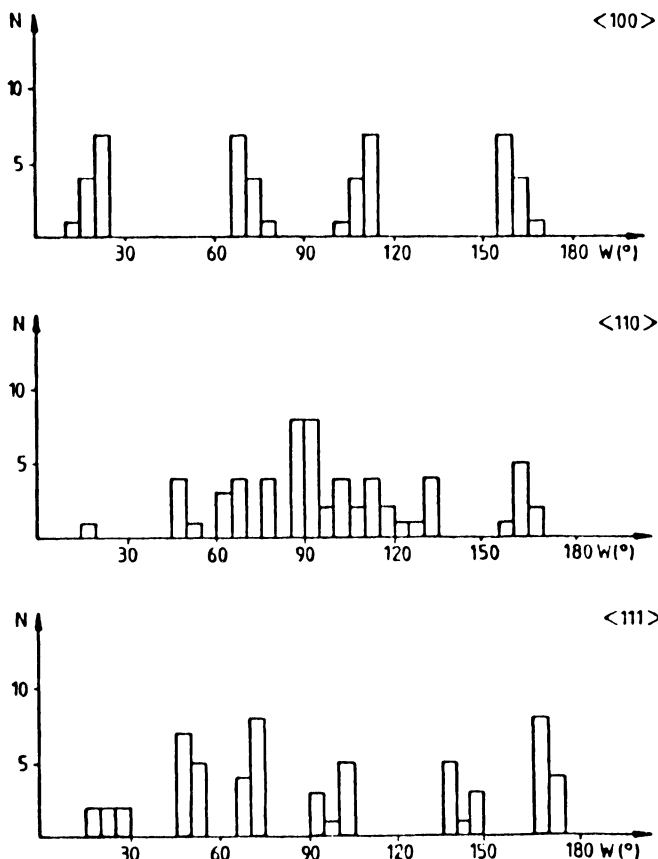


**Figure 4**  $\langle 100 \rangle$ -specimens: frequency distribution of the rotation angles for rotations about the three idealized axes. Only those cases are represented with a deviation of less than  $10^\circ$  between the rotation axis and the ideal direction.

instead of the  $\langle 110 \rangle$ -axis, rotation angles near  $130^\circ$  are mostly found. In summary, 93% of the observed orientation relationships can be described by one of the following rotations:  $20^\circ \langle 100 \rangle$ ,  $20^\circ \langle 111 \rangle$ ,  $50^\circ \langle 111 \rangle$  and  $130^\circ \langle 430 \rangle$ .

The fractions  $h$  of the four orientation relationships are listed in Table 2. The average misorientation between the observed orientation relationships and the idealized ones is only  $6^\circ$ . In the following,

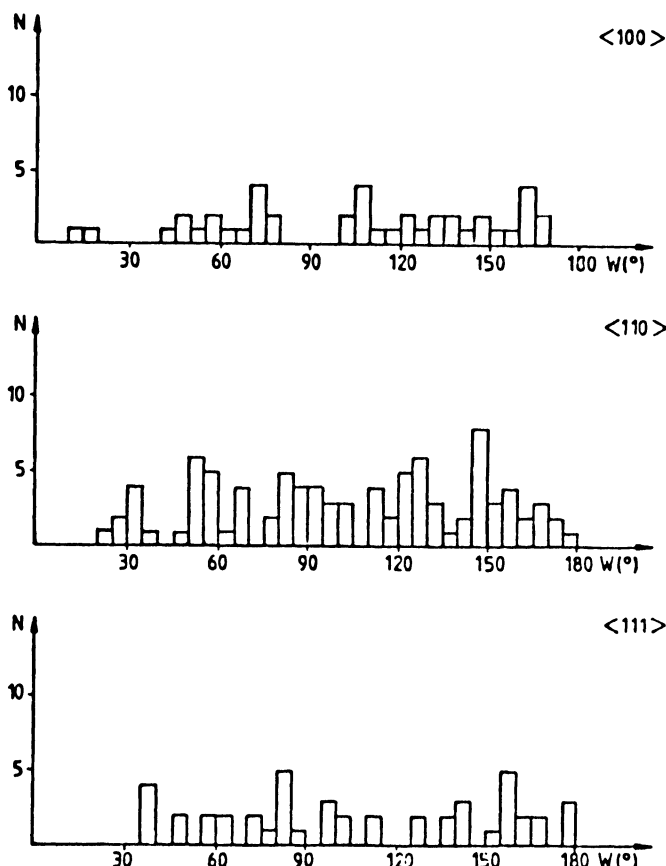


**Figure 5**  $\langle 111 \rangle$ -specimens: frequency distribution of the rotation angles for rotations about the three idealized axes. Only those cases are represented with a deviation less than  $10^\circ$  between the rotation axis and the ideal direction.

the misorientation is used to characterize the deviation between the observed and idealized orientation relationships. The deviation between the observed and the idealized rotation axis describes only the angular distance between the rotation axes, the differences of the rotation angles are not taken into account. Generally, the misorientation is defined as the description of an orientation difference by the smallest possible rotation angle. If the misorienta-

**Table 1** Most frequently occurring angles for the three idealized rotation axes. Taking into account the cubic crystal symmetry the rotation angles in the second column can be replaced by the values given in the third column

$\langle 100 \rangle$ -oriented specimens:

Idealized rotation axis	Rotation angles [°]	Crystallographically equivalent rotation angles [°]
$\langle 100 \rangle$	20, 70, 110, 160	20
$\langle 110 \rangle$	70, 90, 110, 130, 160	20, 50, 70, 90
$\langle 111 \rangle$	20, 50, 70, 100, 140, 170	20, 50

$\langle 111 \rangle$ -oriented specimens:

Idealized rotation axis	Rotation angles [°]	Crystallographically equivalent rotation angles [°]
$\langle 100 \rangle$	15, 45, 55, 75, 105, 125 135, 145, 165	15, 35, 45
$\langle 110 \rangle$	35, 55, 70, 80, 90, 100, 110, 125, 145, 165	15, 35, 55, 70, 80, 90
$\langle 111 \rangle$	40, 50, 60, 70, 80, 100, 140, 160, 170, 180	20, 40, 50, 60

tion is used to describe the quality of an approximation it characterizes the error which is made by replacing the observed orientation relationships by an idealized one.

To judge the physical significance of the results in Table 2 they are compared with the fractions of the four orientation relation-types in a sample of 70 randomly generated orientation relationships. Only if the experimentally observed frequencies are sufficiently higher than these expected values, the associated orientation relationships are regarded as "systematically preferred." The

**Table 2**  $\langle 100 \rangle$ -specimens: percentage of the idealized orientations of the total number

Orientation relation-type	Percentage of total number
$20^\circ \langle 100 \rangle$	17.1%
$20^\circ \langle 111 \rangle$	7.1%
$50^\circ \langle 111 \rangle$	18.6%
$130^\circ \langle 430 \rangle$	50.0%

problem consists of determining the probability  $P$  to find a certain number  $Z$  of orientation relation-types in a sample of  $N = 70$  randomly generated orientation relationships. Here  $Z$  is the observed number of an orientation relation-type. As described elsewhere (Kreyszig, 1982) this probability is given by the cumulative distribution function of the binomial distribution:

$$P(Z, N) = \sum_{n=0}^Z \binom{N}{n} K^n (1 - K)^{(N-n)} \quad (1)$$

Here  $K$  denotes the percentage of each of the interesting orientation relation-types in an infinite number of random orientation relationships. This manifold is calculated by a computer programme which evaluates 20,000 random orientation relation-types according to an algorithm recommended by Mackenzie and Thomson (1957). The calculated probabilities to find the observed number  $Z$  of orientation relation-types in the manifold of 70 random orientation relationships are tabulated (Table 3). As can be seen in the table, the probabilities to find the determined fraction or larger ones in a random sample are very small ( $\leq 0.01\%$ ) for  $20^\circ \langle 100 \rangle$ ,  $50^\circ \langle 111 \rangle$  and  $130^\circ \langle 430 \rangle$ . For the  $20^\circ \langle 111 \rangle$ -orientation relationship this cannot be concluded: the probability to find it as frequently or even more frequently in a random orientation distribution, is still 35%.

This result indicates that orientation relationships of the  $20^\circ \langle 100 \rangle$ -,  $50^\circ \langle 111 \rangle$ - and  $130^\circ \langle 430 \rangle$ -type are systematically preferred by the recrystallization process in the  $\langle 100 \rangle$ -specimens.

The orientations of the  $\langle 111 \rangle$ -specimens were evaluated in the same way. The histograms in Figures 4 and 5 show to a certain extent maxima for the same rotation angles. So a description of the orientation relationships by  $20^\circ \langle 100 \rangle$ ,  $20^\circ \langle 111 \rangle$ ,  $50^\circ \langle 111 \rangle$  and

**Table 3**  $\langle 100 \rangle$ -specimens: probability to find the observed number  $Z$  of orientations in a random sample of 70 orientations

Orientation relation-type	Number $Z$	Probability $P$
$20^\circ \langle 100 \rangle$	12	<0.01%
$20^\circ \langle 111 \rangle$	5	35%
$50^\circ \langle 111 \rangle$	13	<0.01%
$130^\circ \langle 430 \rangle$	35	<0.01%

$130^\circ \langle 430 \rangle$  was tried. Yet this idealization characterizes only 33% of the observed orientation relationships even if the maximum misorientation is  $10^\circ$ . Therefore, the evaluation method has to be modified. Instead of the empirically determined ideal orientation relationships an attempt was made to characterize the results by coincidence orientation relationships. Generally, coincidence grain boundaries have special properties. For example, they are highly mobile even in the presence of foreign atoms (Rutter and Aust, 1965). Additionally, some coincidence grain boundaries have a low energy (Hasson *et al.*, 1972; Gleiter and Chalmers, 1972). In other recrystallization experiments near-coincidence orientation relationships between recrystallized grains and deformed microstructure were frequently observed (Berger, 1986; Lücke, 1974). Also it has to be emphasized that the previous four orientation relation-types can be approximated within less than  $5^\circ$  misorientation by coincidence orientation relationships. The results of the attempt to characterize the observed orientation relationships by coincidence relations are listed in Table 4. It turns out that such a characterization is possible in nearly 70% of the orientation relationships. Only those orientation relationships are listed in the table which were found more than once.

The table indicates that the  $129.8^\circ \langle 540 \rangle$  orientation relationship (formerly characterized as  $130^\circ \langle 430 \rangle$ ) occurs frequently as in the  $\langle 100 \rangle$ -specimens. The  $145.7^\circ \langle 541 \rangle$  orientation relationship shows nearly the same frequency of occurrence. The statistical significance

**Table 4**  $\langle 111 \rangle$ -specimens: percentage of the idealized coincidence orientations of the total number

Coincidence orientation relationships		Percentage of the idealized orientation relation-types
$\Sigma$	13a	22.6° $\langle 100 \rangle$
$\Sigma$	21	21.8° $\langle 111 \rangle$
$\Sigma$	19	46.8° $\langle 111 \rangle$
$\Sigma$	25	129.8° $\langle 540 \rangle$
		19.2%
$\Sigma$	23	145.7° $\langle 541 \rangle$
$\Sigma$	19a	26.5° $\langle 110 \rangle$
$\Sigma$	9	38.9° $\langle 110 \rangle$
$\Sigma$	7	38.2° $\langle 111 \rangle$
$\Sigma$	5	36.9° $\langle 100 \rangle$
		2.0%

**Table 5**  $\langle 111 \rangle$ -specimens: probability to find the observed number  $Z$  of orientation in a random sample of 99 orientations

Coincidence orientation relationships		Number $Z$	Probability $P$
$\Sigma 13a$	$22.6^\circ \langle 100 \rangle$	7	15.1%
$\Sigma 21$	$21.8^\circ \langle 111 \rangle$	4	79.8%
$\Sigma 19$	$46.8^\circ \langle 111 \rangle$	3	91.2%
$\Sigma 25$	$129.8^\circ \langle 540 \rangle$	19	12.5%
$\Sigma 23$	$145.7^\circ \langle 541 \rangle$	18	31.0%
$\Sigma 19a$	$26.5^\circ \langle 110 \rangle$	6	85.6%
$\Sigma 9$	$38.9^\circ \langle 110 \rangle$	5	92.6%
$\Sigma 7$	$38.2^\circ \langle 111 \rangle$	4	79.1%
$\Sigma 5$	$36.9^\circ \langle 100 \rangle$	2	91.5%

of the results was determined as described above. The calculated probabilities to obtain the observed results by chance are tabulated, too (Table 5). For the  $\langle 111 \rangle$ -specimens the probabilities to find the observed fractions in a random sample are greater than in the  $\langle 100 \rangle$ -specimens because the corresponding numbers of orientation relationships of one type are smaller.  $22.6^\circ \langle 100 \rangle$ ,  $129.8^\circ \langle 540 \rangle$  and  $145.7^\circ \langle 541 \rangle$  have a probability appreciably less or near equal to 30%. Compared with the other observed orientation relationships, however, their occurrence is clearly more significant. The fractions of orientation types of the 88 orientation relationships in the second kind of  $\langle 100 \rangle$ -specimens are summarized in Table 6. As in the first charge of  $\langle 100 \rangle$  crystals also in these specimens the four

**Table 6**  $\langle 100 \rangle$ -specimens of the second kind: probability to find the observed number  $Z$  of orientations in a random sample of 88 orientations

Orientation relation-type		Number $Z$	Probability $P$
$\Sigma 13a$	$22.6^\circ \langle 100 \rangle$	14	2.0%
$\Sigma 21$	$21.8^\circ \langle 111 \rangle$	9	5.8%
$\Sigma 19$	$46.8^\circ \langle 111 \rangle$	8	11.0%
$\Sigma 25$	$129.8^\circ \langle 540 \rangle$	30	$5 \cdot 10^{-4}\%$
$\Sigma 23$	$145.7^\circ \langle 541 \rangle$	8	97.9%
$\Sigma 19a$	$26.5^\circ \langle 110 \rangle$	6	76.9%
$\Sigma 9$	$38.9^\circ \langle 110 \rangle$	6	75.8%
$\Sigma 7$	$38.2^\circ \langle 111 \rangle$	3	86.7%
$\Sigma 5$	$36.9^\circ \langle 100 \rangle$	3	68.6%

orientation relation-types:  $22.6^\circ \langle 100 \rangle$ ,  $21.8^\circ \langle 111 \rangle$ ,  $46.8^\circ \langle 111 \rangle$  and  $129.8^\circ \langle 540 \rangle$  dominate. They occur with a significant frequency. All additional orientation relationships fit the system of orientation relation-types of the  $\langle 111 \rangle$ -specimens.

Additionally, the areas covered by grains belonging to the different orientation relation-types were determined in  $\langle 100 \rangle$ - and  $\langle 111 \rangle$ -oriented specimens. It turns out that on the average the fractions of areas coincide with the corresponding fractions of orientations of the total number investigated. So it is concluded that in both types of specimens for all orientation relation-types the average area per grain is the same.

## DISCUSSION

The results described in the previous section indicate that in all crystals the two orientation relationships  $22.6^\circ \langle 100 \rangle$  and  $129.8^\circ \langle 540 \rangle$  occur with a significant frequency. The main difference between the first set of  $\langle 100 \rangle$ -specimens and the set of  $\langle 111 \rangle$ -specimens is the sharpness of the orientation distribution. This observation is interpreted as resulting from the different dislocation densities. As mentioned above, in the deformed  $\langle 111 \rangle$ -oriented crystals the dislocation density is about five times smaller than in the  $\langle 100 \rangle$ -oriented crystals. Form and co-workers (1980) demonstrated that the annealing twin density increases with the dislocation density. Moreover, the smaller dislocation density in the  $\langle 111 \rangle$ -oriented crystals causes a smaller driving force for the recrystallization process. So our conclusion is that the recrystallized microstructure in these crystals represents an early stage of the process. This hypothesis is confirmed by the results of the additional experiments with  $\langle 100 \rangle$ -oriented crystals grown from the second charge of copper. In these specimens the observed orientation relationships can be well characterized by the system of orientation relation-types used for the  $\langle 111 \rangle$  specimens. Yet the distribution is shifted to the four orientation relation-types observed in the other  $\langle 100 \rangle$ -specimens. A further analysis of the orientations yields that in 5 cm distance from the abraded end, i.e. the nucleation region, 80% of all orientation relationships belong to the types  $22.6^\circ \langle 100 \rangle$ ,  $21.8^\circ \langle 111 \rangle$ ,  $46.8^\circ \langle 111 \rangle$  and  $129.8^\circ \langle 540 \rangle$ . In this region the

orientations of the recrystallized microstructure correspond to those of the  $\langle 100 \rangle$ -crystals of the first kind. Summarizing, the  $\langle 100 \rangle$ -crystals of the second type represent the transition from the distribution of orientation relationships of the  $\langle 111 \rangle$ -crystals to that of the  $\langle 100 \rangle$ -crystals of the first kind.

This result indicates also, that the recrystallization process depends very sensitively on small variations of the impurity content. As mentioned above, the only difference between the two kinds of  $\langle 100 \rangle$ -crystals is the raw material which comes from different charges of the same nominal purity.

The numerous annealing twins in the recrystallized microstructure (Figure 3) elucidate the role of twinning in the recrystallization process. The recrystallization process in our specimens can be divided into three stages. First, after random nucleation twinning leads to the formation of a large number of orientations. Yet this process does not occur at random. The decrease of interfacial energy caused by the orientation change is the controlling mechanism. It leads to the preferred formation of orientations with a low interfacial energy. There is now experimental evidence supporting this idea. Berger (1986) observed in his HVEM recrystallization experiments the formation of small angle grain boundaries by twinning. Additionally, in this stage twinning may lead also to the formation of orientation relationships suitable for rapid grain growth. The second stage of the recrystallization process is characterized by an optimization process between formation of grain boundaries of low interfacial energy and of high mobility. Those orientations will dominate in this stage which have an optimum ratio between these two parameters. A small grain boundary energy guarantees a stability against further twinning. But the grain boundary mobility must be sufficiently large. Otherwise the grains will be left behind. In the third stage further growth of the dominating orientations takes place. Yet, occasionally, back-twinning may occur if the interfacial energy differences between the two orientations are small.

The  $145.7^\circ \langle 541 \rangle$  orientation relationship is assigned to the first stage because it was not observed in the  $\langle 100 \rangle$ -specimens of the first kind. A further investigation of the relations between the  $145.7^\circ \langle 541 \rangle$  orientation relationship and the four finally dominating orientation relation-types shows that in all cases a connection by

twin chains is possible. Always the orientation with the  $145.7^\circ \langle 541 \rangle$  relation turns out as starting link. The  $129.8^\circ \langle 540 \rangle$  orientation relationship is explained as first order twin of the  $145.7^\circ \langle 541 \rangle$  orientation relationship. The  $21.8^\circ \langle 111 \rangle$  can be approximated by a second order twin. Twin chains over three generations are necessary for near  $22.6^\circ \langle 100 \rangle$  and  $46.8^\circ \langle 111 \rangle$  orientation relationships. A deviation of less than  $5^\circ$  between calculated and ideal rotation axis has to be allowed.

Experimental evidence for the twin relationship between  $145.7^\circ \langle 541 \rangle$  and  $129.8^\circ \langle 540 \rangle$  was found in our specimens. Often, in grains with a  $129.8^\circ \langle 540 \rangle$  orientation relationship fine twin lamellae were formed. The twin lamellae have a  $145.7^\circ \langle 541 \rangle$  orientation relationship to the deformed microstructure and are thin relative to the dimension of the grains. The observed multiple twinning and backtwinning is favoured by the small difference in interfacial energy between the two orientations. The different thickness of the regions belonging to the two orientations reveal a smaller growth capacity of the  $145.7^\circ \langle 541 \rangle$  orientation relationship. Thus, the dominance of grains with a  $129.8^\circ \langle 540 \rangle$  orientation relationship is the result of their larger growth capacity.

Moreover, on the basis of this model the minor role of the  $38.2^\circ \langle 111 \rangle$  orientation relationship in our experiments becomes understandable. This orientation relationship was observed in the  $\langle 111 \rangle$ -specimens in 4% of all cases. In the  $\langle 100 \rangle$ -specimens of the second kind it could be detected only near the nucleation region. Generally, the  $38.2^\circ \langle 111 \rangle$ -orientation relationship is known as favouring rapid grain growth (Liebmann *et al.*, 1956). The disappearance of the  $38.2^\circ \langle 111 \rangle$  orientation relationship in our experiments leads to the conclusion that this orientation has only a limited stability against further twinning. This is in accordance with HVEM-observations and texture measurements in aluminium (Berger, 1981). According to these results one prerequisite for the observation of the  $38.2^\circ \langle 111 \rangle$  orientation relationship in a recrystallization texture is a suitable morphology of the deformed microstructure. Whenever there are many nucleation sites distributed within the whole microstructure the growth process cannot proceed over large distances. Under these circumstances only the first or second stage of our model can be observed. This favours the occurrence of grains

**Table 7** Idealization of the calculated orientation relationships between the components of the deformation texture and the recrystallization texture of polycrystalline copper

Components of the deformation texture	Component of the recrystallization texture	Idealization by coincidence orientation relationship (misorientation)
(112) [11̄1]	(001) [100]	129.8° ⟨540⟩ (8°)
(011) [21̄1]	(001) [100]	129.8° ⟨540⟩ (8°)
(123) [63̄4]	(001) [100]	46.8° ⟨111⟩ (5°)
(013) [100]	(001) [100]	22.6° ⟨100⟩ (4°)

with a  $38.2^\circ \langle 111 \rangle$  orientation relationship in the recrystallized microstructure.

Finally, the importance of the four dominating orientation relationships for polycrystalline material can be estimated on the basis of the orientation relationships between the dominating components of the copper deformation and -recrystallization texture. According to Schmidt (1975) the deformation texture of rolled copper can be characterized by the three dominating components (112) [11̄1], (011) [21̄1] and (123) [63̄4] and a weaker one (013) [100]. The recrystallized material shows the cube recrystallization texture (001) [100]. All orientation relationships are listed in Table 7. In all cases they can be idealized by one of the orientation relationships found in our experiments. The misorientation resulting from this idealization is not more than  $8^\circ$ .

## CONCLUSIONS

The described results clearly demonstrate that there is more than one orientation relationship necessary to characterize the preferred orientations of the recrystallized microstructure. Despite the simplicity of the experiments the results can help to describe more accurately the orientation relationships between the deformation texture and the recrystallization texture. Thus, the model experiments are suitable to get a better understanding of the processes controlling recrystallization texture formation in polycrystalline materials.

## Acknowledgement

The authors are indebted to Prof. Dr. P. Haasen for the encouraging support of these investigations, many helpful discussions and critical comments on the manuscript.

## References

- Ambrosi, P., Göttler, E. and Schwink, Ch. (1974). *Scripta Met.* **8**, 1093–1098.
- Berger, A. (1981). Diploma Thesis, Göttingen.
- Berger, A. (1986). Doctoral Thesis, Göttingen.
- Form, W., Gindraux, G. and Mlynkar, V. (1980). *Met. Sci. J.* **14**, 16–20.
- Gleiter, H. and Chalmers, B. (1972). in *Progress in Material Science* **16**, edit. Chalmers, B., Christian, J. W. and Massalski, T. B., Pergamon Press.
- Göttler, E. (1973). *Phil. Mag.* **28**, 1057–1076.
- Gottstein, G. (1978). in *Textures of Materials* (I + II), edit. Gottstein, G. and Lücke, K., Springer Verlag.
- Hasson, G., Herbeval, I., Bicondi, M. and Goux, C. (1972). in Proceedings of the International Conference of the Structure and Properties of Grain Boundaries and Interfaces, edit. Chaudhari, P. and Matthews, J. W., North Holland Publishing Company, Amsterdam.
- Kreyszig, E. (1982). *Statistische Methoden und ihre Anwendung*, Vandenhoeck und Ruprecht, Göttingen.
- Liebmamn, B., Lücke, K. and Masing, G. (1956). *Z. Metkde.* **47**, 57–63.
- Lücke, K. (1984). in Proceedings ICOTOM 7, pp. 195–210, edit. Brakmann, C. M., Jongenburger, P. and Mittemeijer, E. J., Netherlands Society of Materials Science, Zwijndrecht, Holland.
- Lücke, K. (1974). *Can. Met. Quarterly* **13**, 261–273.
- Mackenzie, J. K. and Thomson, M. J. (1957). *Biometrika* **44**, 205–213.
- Pfeiffer, K. (1964). Diploma Thesis, München.
- Plege, B. (1986). in Proceedings of the 7th International Symposium on Metallurgy and Material Science, pp. 493–501, edit. Hansen, N., Juul Jensen, D., Leffers, T. and Ralph, B., Risø National Laboratory.
- Rutter, J. W. and Aust, K. T. (1965). *Acta Met.* **13**, 181–186.
- Schmidt, U. (1975). Doctoral Thesis, Aachen.
- Vorbrugg, W., Goetting, H. Ch. and Schwink, Ch. (1971). *Ch. phys. stat. sol. (b)* **46**, 257–264.
- Wilbrandt, P.-J. (1978). Doctoral Thesis, Göttingen.
- Wilbrandt, P.-J. and Haasen, P. (1980). *Z. Metkde.* **71**, 385–395.